EVALUATION METHODS TO DETERMINE SOIL AND WATER CONSERVATION STATUS IN DIFFERENT ECOSYSTEMS

Xin Li¹, Lu Zhao^{1*}, Guoqing Cui^{1,2}, Liangli Li³, Tingyu Zhang⁴ and Shan Liu⁴

The First Topographic Surveying Brigade of Ministry of Natural Resource of P.R.C., Xi'an 710054, China

Keywords: Ecosystem, Water and soil conservation, Functional evaluation, GIS

Abstract

In order to study the effect of different vegetation types on ecosystem water and soil conservation function, an area was selected as the research object, and the evaluation method of ecosystem water and soil conservation function under the application of different plant measures was designed based on ENVI and ArcGIS software. Delineate five types of vegetation in the study area. The experimental results showed that in the evaluation of water conservation function, the water conservation capacity of the five types of vegetation and the water conservation amount per unit area are ranked from large to small, *i.e.* grassland, shrub grassland, woodland, woodland and shrub mixed areas, cultivated land, in the evaluation of soil water conservation function, the potential and actual soil erosion of cultivated land are much greater than those of the other four vegetation types. Among the remaining four vegetation types, shrubs > mixed area of shrubs and forest land > forest land > grassland. In the order of soil conservation per unit area, cultivated land is far less than other vegetation types, and the other orders are grassland > forest land > mixed area of forest land and shrub > shrub. It can be seen that among the five vegetation types, grassland has the strongest effect on soil and water conservation, and cultivated land is the worst.

Introduction

In the study of soil and water conservation, vegetation has consistently played a pivotal role. Through the implementation of vegetative measures, the surface of the research area becomes increasingly covered by plant life, significantly reducing surface roughness. This, in turn, enhances both the soil's water retention capacity and its porosity. As a result, when rainfall occurs, water does not merely flow across the surface as runoff, stripping away the topsoil. Instead, a substantial portion of the precipitation infiltrates the soil, thereby boosting its moisture-holding capacity and preserving the integrity of both soil and water. To evaluate the efficacy of such vegetative approaches in sustaining soil and water within a given ecosystem, a fundamental assessment methodology has been devised.

GIS technology was employed to extract essential data on precipitation, soil, and vegetation cover related to the ecosystem's soil and water conservation functions within the study area (Jin 2019). Based on this, an elevation map was constructed, and the soil retention capacity of the region was estimated using a soil erosion equation. A classification standard was established, and a comprehensive evaluation of the area's soil and water conservation function was conducted. A soil erosion modeling, forest health assessment and quantitative assessment method for the soil and water conservation capacity of an artificially constructed shrub-grass ecosystem were proposed in relevant research (Sing *et al.* 2014, Momdal *et al.* 2015, Liu *et al.* 2021). Centered around the IVEST model, it introduced a theoretical framework for the sustainable development of soil and

^{*}Author for correspondence: <598308919@qq.com>. ¹The First Topographic Surveying Brigade of Ministry of Natural Resource of P.R.C., Xi'an 710054, China. ²Northwest Land and Resources Research Center, Shaanxi Normal University, Xi'an 710119, China. ³College of Land Engineering, Chang'an University, Xi'an 710054, China. ⁴Shaanxi Agricultural Development Group Co., Ltd., Xi'an 710075, China

water resources within the study region. Experimental data confirmed that artificial shrub-grasslands possess considerable soil and water conservation capabilities, contributing significantly to the ecological preservation of the area. In a prior investigation, six forestland types distributed throughout the whole regional scope were chosen as research subjects for evaluating the effectiveness of soil and water conservation (Lou *et al.* 2025). Through on-site observation and analysis of their water retention capacity, a relatively accurate method for assessing the water conservation function of forest ecosystems was established. Experimental data on soil porosity and effective water-holding capacity were used to identify the forest type with the strongest water retention performance. This paper proposes a novel evaluation method for assessing the ecological soil and water conservation function, grounded in vegetative measures, to assess the current state of conservation across different areas within the study region.

The region depicted in Fig. 1 was selected as the study area for this experiment, encompassing a total area of approximately 1,723 Km². The maximum elevation reaches 623 meters, while the lowest point lies around 135 meters above sea level. The area is traversed by several rivers, ensuring an abundant supply of water resources. Rich in diverse vegetation, the ecosystem exhibits a well-developed capacity for soil and water conservation (Guo *et al.* 2024).

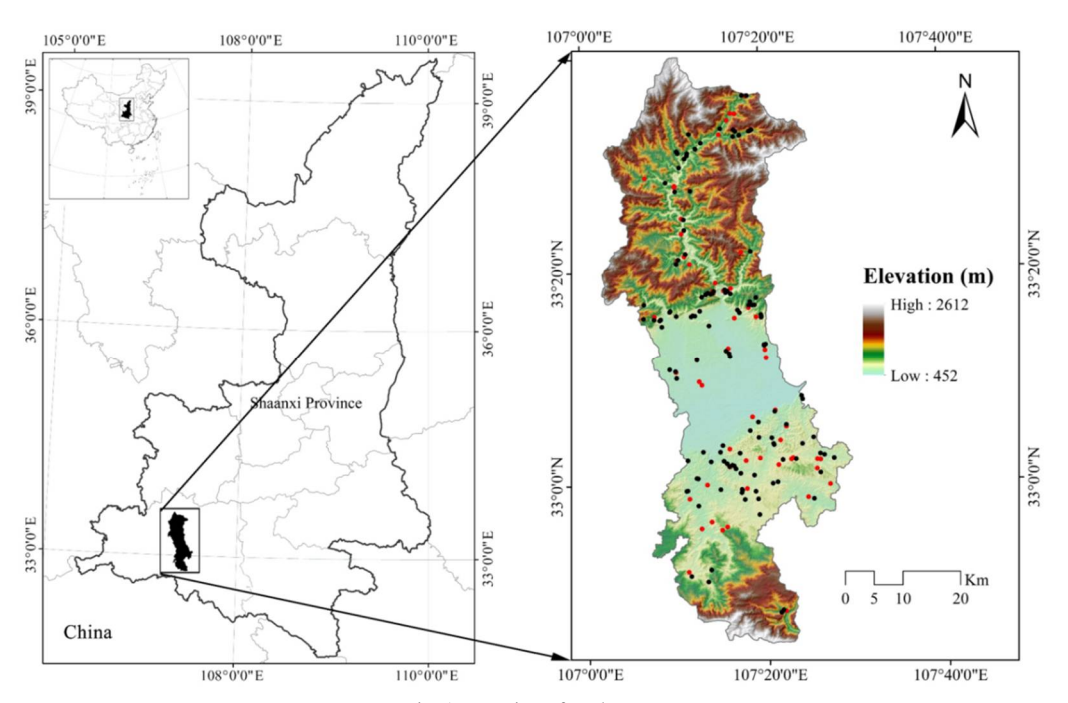


Fig. 1. Location of study area.

During the acquisition and preprocessing of experimental data, remote sensing information was primarily obtained using ENVI technology, followed by image preprocessing with ArcGIS. Field surveys were then conducted to identify the types of vegetation cover across various plots within the study area (Qiu *et al.* 2023). The land is predominantly vegetated. Essential data required in this process included the topographic map of the study area as shown in Fig. 1, land use survey results, satellite imagery of vegetation cover, and regional precipitation data. Landsat imagery was selected from the Geospatial Data Cloud as the source of remote sensing data and

imported into ENVI for geometric correction and color enhancement, allowing the distinct boundaries of structural features to be clearly delineated (Bilal *et al.* 2025). The images were then subjected to supervised classification to achieve a spatial resolution of 20 meters (Liu *et al.* 2023). Through the interpretation of the remote sensing imagery, a schematic vegetation cover map, as illustrated in Fig. 2, was derived.

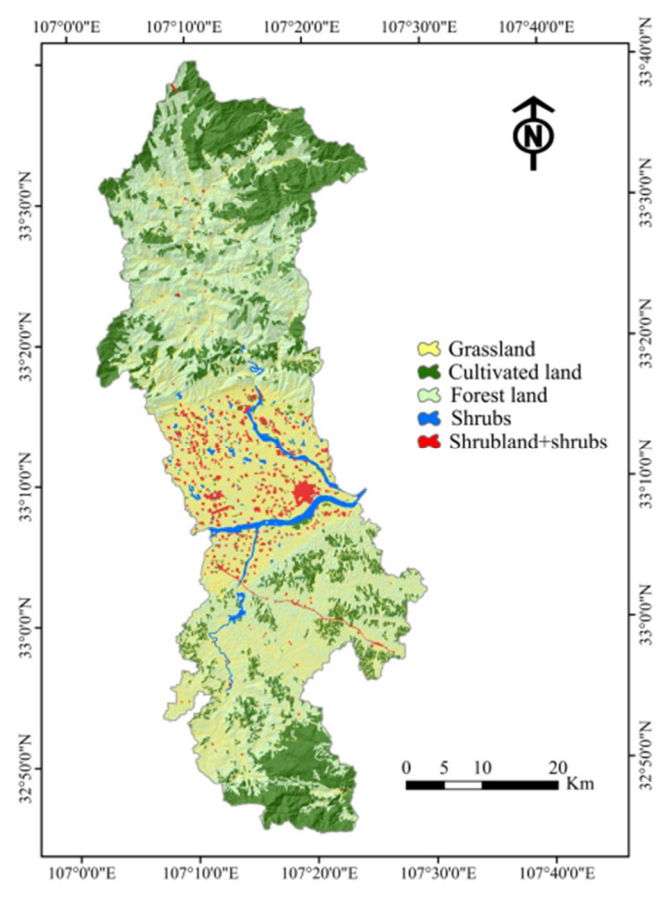


Fig. 2. Vegetation coverage of the study area.

As illustrated in Fig. 2, following the acquisition of remote sensing imagery via ENVI, the land was broadly classified into five categories: grassland, woodland, shrubland, cultivated land, and mixed forest-cultivated land (Yang *et al.* 2022). Prior to this, it was essential to convert the collected information and data into compatible formats to ensure seamless integration and accessibility within the ArcGIS platform. In ArcGIS, a minimum of three layers, each derived from distinct image sources, must be established. To minimize image distortion, all coordinate systems were standardized, with the 1980 Xi'an Coordinate System selected as the unified reference frame for this study(Chen *et al.* 2020). Land use data was rasterized at 1 km intervals, superimposed using ArcGIS, and used to calculate the annual Normalized Difference Vegetation Index (NDVI) (Zhang *et al.* 2021). At this stage, soil and moisture data could be integrated into the remote sensing images. Hydrological information was extracted using a gridding method, and a Digital Elevation Model (DEM) was subsequently constructed.

Using the aforementioned DEM data and regional vegetation coverage map as the foundational input, the analytical formulas were integrated into the ArcGIS software for comprehensive analysis. The first step involved constructing a water conservation capacity model based on regional precipitation data and vegetation distribution (Dongyang *et al.* 2019). By accounting for rainfall and plant transpiration, the soil water yield for a given area was calculated. Subsequently, parameters such as root depth and soil type were incorporated into the model for calibration. Finally, by combining topographical features, soil water saturation, and subsurface flow velocity, the water conservation capacity of the region was computed. The corresponding calculation formula is as follows.

$$V_{water} = (1 - \frac{\lambda_e}{V_{vear}}) \times V_{year}$$
 (1)

In the equation: V_{water} denotes the annual volume of water produced by the soil within the study area; V_{year} represents the region's average annual precipitation; λ_e signifies the mean annual transpiration for each grid cell. The ratio λ_e/V_{year} can be derived using Equation (2).

$$\frac{\lambda_e}{V_{vear}} = 1 + \frac{\gamma_e}{V_{vear}} - \left[1 + \left(\frac{\gamma_e}{V_{vear}}\right)^9\right]^{\frac{1}{9}} \tag{2}$$

In the equation, γ_e denotes the mean annual potential evapotranspiration for each grid unit, while θ represents the soil property parameter specific to the region. The formula for calculating γ_e is thus expressed as follows.

$$\gamma_e = \theta_{pla} \times \mu_e \tag{3}$$

In the equation: θ_{pla} denotes the vegetation cover coefficient for a specific area within the study region, while μ_e represents the reference evapotranspiration for each individual grid cell. By applying the above formulas holistically, the regional water conservation coefficient can thus be derived.

$$\rho_{water} = \min(1, \frac{336}{n_{x}}) \times \min(1, \frac{0.37 \times \chi_{dx}}{2.62}) \times \min(1, \frac{\pi_{td}}{257}) \times V_{water}$$
(4)

In the equation, ρ_{water} represents the water conservation parameter for a given area; η_x denotes the groundwater flow coefficient; χ_{dx} refers to the topographic elevation factor, indicating relative altitude; and π_{td} signifies the soil saturated water flow coefficient under vegetation-based interventions. The above constitutes the method for calculating the water conservation coefficient. In addition to this, vegetation measures also significantly influence the soil's capacity for moisture retention (Wang and Liu 2023). This process requires a comprehensive consideration of various factors, including terrain features, vegetation cover, meteorological precipitation conditions, and soil composition. The principal formula is as follows.

$$S_{a} = \sum_{i=1}^{n} (R_{a} - U_{a}) _sed_{ex}$$
 (5)

In the equation, S_a denotes the soil retention coefficient of the study area under the influence of precipitation; R_n represents the volume of soil on the verge of erosion under a given level of rainfall; U_n indicates the quantity of soil that has already been lost under the same conditions; and

 sed_{ex} refers to the volume of sediment intercepted by the land from upstream sources. The formulas for calculating R_n and U_n are as follows.

$$\begin{cases} R_a = r_a \times k_a \times s_a \\ U_a = r_a \times k_a \times s_a \times h_a \times p_a \end{cases}$$
 (6)

In the equation, r_a represents the annual average precipitation coefficient; k_a denotes the erosion factor of the specific soil type; s_a signifies the average slope coefficient of the region; h_a refers to the vegetation cover and management coefficient; and p_a indicates the coefficient related to soil conservation practices. By integrating the aforementioned equations and inputting the data into the DEM imagery within ArcGIS, the precise soil and water conservation parameters for a given region can be effectively determined.

During the preprocessing of imagery, initial datasets such as topographic maps of the study area, land use survey results and imagery, satellite vegetation cover images, and regional annual average precipitation data are obtained (Yang *et al.* 2024). Following field surveys and manual investigations, these images yield detailed and reliable data, which serve as critical inputs for this study. In field research, the most essential metric is the soil moisture content within specific regions. To this end, soil monitoring points must be established on both the sunny and shaded slopes of the study area. Using time domain reflectometry, moisture levels within the soil layers are measured, with data checked at 10-day intervals to ensure accuracy in capturing subsurface water flow.

Within ArcGIS, watershed boundaries and precipitation erosion potential are extracted and transformed into DEM data (Cohen *et al.* 2024). The annual average precipitation is then interpolated into spatial grid datasets, and water loss due to transpiration is calculated under corresponding temperature and sunlight conditions. The spatial resolution at this stage is approximately 20 meters. Upon obtaining reference values for water conservation and soil retention functions, evaluations are conducted under various vegetation scenarios to assess the ecological effectiveness of each plant type.

Results and Discussion

Within the study area, the 1,723 km² of land can be categorized into five distinct vegetation-based land types: cultivated land, grassland, forest land, shrub-grassland, and mixed zones of forest and shrub. Cultivated land is predominantly concentrated in the central region, where the river network is densest. This area is characterized by relatively low elevation and minimal relative height, and cultivated land generally exists independently of other land types. Grassland is scattered across various corners of the study area. The grasslands marked in Fig. 2 represent pure grassland, though herbaceous plants are also found in forested zones, shrubland, and their transitional areas. Shrublands, also referred to as shrub-grasslands, are areas where dense shrub clusters grow within grasslands, typically found on steeper slopes. Forest land refers to regions dominated by tall, woody vegetation-mostly trees-often interspersed with herbaceous undergrowth. The mixed forest-shrub zones are areas where both trees and shrubs coexist, generally located at higher altitudes.

Calculations reveal that these five land types significantly influence soil moisture content, with varying capacities for water retention and conservation. By applying Formula (4) within ArcGIS, the impact of each land type on water conservation functions is evaluated, producing the spatial distribution map of the study area's water conservation capacity, as depicted in Fig. 3.

The spatial distribution of water conservation functions under different vegetation measures is illustrated in Fig. 3. When analyzed in conjunction with Fig. 2, the evaluation results of water

conservation capacity for each vegetation type are presented in Table 1. As shown, among the five vegetation categories, the overall ranking of water conservation capacity and per-unit-area water retention, from highest to lowest, is as follows: grassland, shrub-grassland, forest land, mixed forest and shrubland, and finally, cultivated land. Based on the per-unit-area water retention results calculated with respect to the total land area of the study region, grassland exhibits the greatest capacity, followed by mixed forest and shrub zones, shrub-grassland, and forest land, with cultivated land demonstrating the lowest capacity for water conservation.

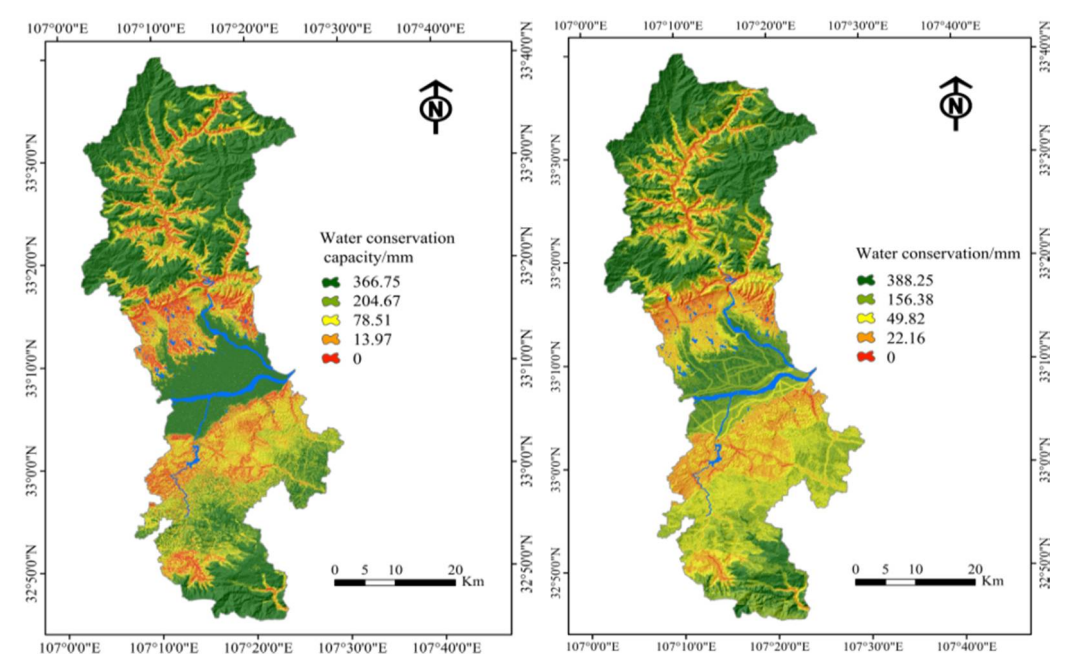


Fig. 3. Spatial distribution of water conservation function.

Table 1. Assessment of water conservation function of various vegetation types.

	Grassland	Cultivated land	Forest land	Shrubs	Shrub land + Shrubs
Land area/km ²	628.34	656.47	225.43	156.77	55.99
Water conservation capacity/mm	36.25	30.08	30.26	30.79	30.14
Total water conservation capacity/m ²	5962.31×10 ⁴	1929.26×10 ⁴	1062.37×10 ⁴	965.29×10 ⁴	559.38×10 ⁴
Unit area water conservation capacity/m ² ·hm ⁻²	948.88	293.88	471.26	615.73	999.07

The impact of various vegetation types on soil moisture retention, as derived from Equations (5) and (6), is illustrated in Fig. 4. The spatial distribution of soil conservation functions under different vegetation measures is also presented in Fig. 4. When examined alongside the vegetation classification map in Fig. 2, the corresponding evaluation results are detailed in Table 1.

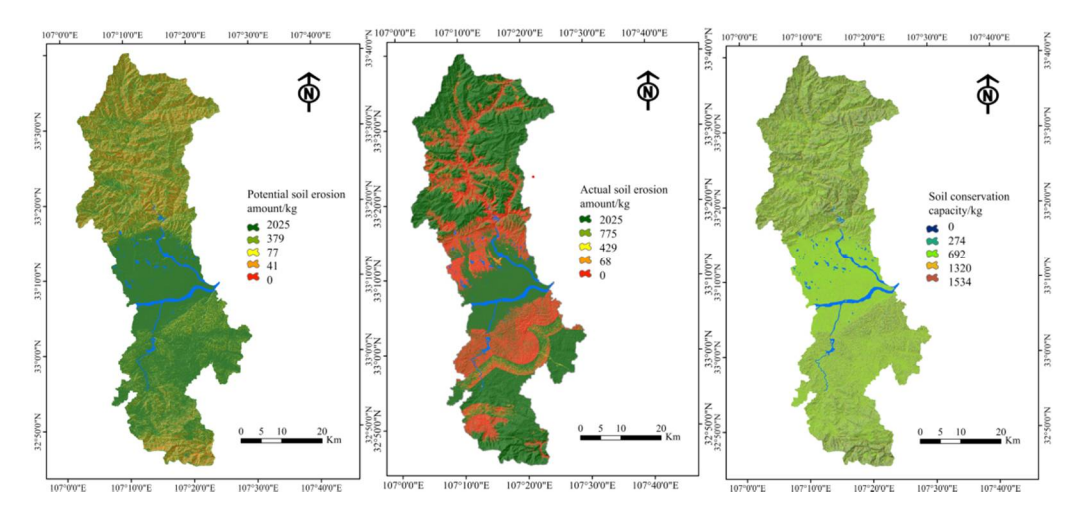


Fig. 4. Spatial distribution of soil conservation function.

In the comparison of potential versus actual soil erosion across the five vegetation types, cultivated land exhibits significantly higher values than the others. Among the remaining types, the descending order is shrubland, mixed shrub-forest zones, forest land, and grassland. In terms of total soil retention, grassland ranks highest, followed by forest land, mixed shrub-forest areas, shrubland, and lastly, cultivated land.

Synthesizing the findings of the two assessments-focused on evaluating the ecosystem's water and soil conservation functions- it is evident that the effectiveness of different vegetation types varies considerably. Grassland proves to be the most efficient in achieving water and soil conservation, whereas cultivated land performs the poorest in this regard.

In this study, grassland, cultivated land, forest land, shrub-grassland, and mixed zones of forest and shrub-grassland were classified as distinct vegetation types, and their respective roles in water and soil conservation were individually assessed. According to the experimental findings, grassland exhibited the most effective conservation performance, while cultivated land proved the least effective. It is worth noting that the evaluation was conducted under the assumption of ideal rainfall and climatic conditions, without accounting for extreme weather events. Therefore, future research should incorporate such scenarios for a more comprehensive analysis.

Acknowledgements

The work was funded by The National Natural Science Foundation of China (NSFC) (Grant No. 42401434); Shaanxi Province Youth Science and Technology Rising Star Project (2025ZCKJXX-148); State Key Laboratory of Spatial Datum (No. SK LSD2025-KF-09); Key Research and Development Program of Shaanxi (Program No. 2024SF-YBXM-565); Natural Science Basic Research Program of Shaanxi (2025JC-YBMS-334); The Fundamental Research Funds for the Central Universities, CHD (300102355201); Internal research projects of Shaanxi Agricultural Development Group (NFJC2025- 55, NFJC2025-56, NFJC2025-57) Inner scientific research project of Shaanxi Land Engineering Construction Group (DJNY2023-16, DJNY2023-18, DJNY2023-33, DJHZKY202402).

References

Bilal H, Lahlou FZ and Al-Ansari T 2025. Land suitability assessment and self-sufficiency evaluation for fodder crop production in a hyper arid environment coupling GIS-based multi-criteria decision making and optimization. Ecol. Mode. **501**(22): 36-49.

- Chen Y, Gong A, Zeng T and Yang Y 2020. Evaluation of water conservation function in the Xiongan New Area based on the comprehensive index method. PLoS ONE **15**(9): 238-255.
- Cohen JG, Enander HD, Bassett TJ, Wilton CM and Cole-Wick AA 2024. Using GIS-based multicriteria decision analysis to prioritize invasive plant treatment: A creative solution for a pernicious problem. Ecol. Mode. **495**(10): 21-40.
- Dongyang XU, Yongtai R, Kun C and University NA 2019. Screening and application of ecological security indicators for regional soil and water resources. Environ. Sci. Technol. 7(2): 907-1008.
- Guo S, Zheng PS, Tang Y, Leng LH and Li SC 2024. Analysis of fluid flow characteristics in spherical nonlinear seepage flow model for dual-porous reservoir with the elastic outer boundary. Acta Geophysica 72(5): 3179-3189.
- Jin XU 2019. Static characteristics analysis of ecological reinforced retaining wall of river embankment based on physical model test. Ground Water **32**(14): 99-112.
- Liu B, Ye W, Zhu C, Chen R and Ni X 2021. Analysis on Treatment Effect of Mine Tunnel Construction Spring in Karst Area. Math. Prob. Eng. 2021(3): 1-11.
- Liu Y, Gao Y, Fu Y, Xu Z, Li Q and Wang H 2023. A framework of ecological sensitivity assessment for the groundwater system in the Mi River basin, Eastern China. Environ. Earth Sci. 18(21): 309-327.
- Lou S, Chen S, Yang Z, Zhang Z, Liu S and Fedorova IV 2025. Seasonal Effects of Hydrometeorological Factors on the Distribution and Partition of Organic Carbon in the Yangtze River Estuary. Estuar. Coast. **48**(4): 746-758.
- Mandal UK, Dutta S, Nazma, Ali MS, Sharifee NM and Ahmed A 2015. Spatial soil erosion modeling for sustainable agriculture development using remote sensing and GIS technology. Dhaka Univ. J. Biol. Sci. **24**(2): 177-189, (July)
- Qiu Q, Duan Y, Ma K, Tao L and Xie Z 2023. Information extraction and knowledge linkage of geological profiles and related contextual texts from mineral exploration reports for geological knowledge graphs construction. Ore Geol. Rev. **163**(1): 14-34.
- Singh D, Singh S, Lekshmi VR, Dutta S, Nazma, Ali MS, Ahmed A 2014. Species Type and Forest Health Assessment via Hyperspectral Remote Sensing in the part of Himalayan Range, India. Dhaka Univ. J. Biol. Sci. 23(2): 135 146 (July).
- Wang J and Liu T 2023. Region selection and efficiency improvement for apple production using an indicator system based on cost-effective factors. Int. J. Agricul. Sustain. 21(1): 25-45.
- Yang B, Zhang T, Tian J, Li J and Feng P 2024. Ecological risk assessment in the Ziya watershed under the influences of land use change and water resource shortage. Catena **244**(000): 16-33.
- Yang Y, Liu H and Li SLW 2022. Planting in ecologically solidified soil and its use. Open geosci. **14**(1): 750-762.
- Zhang Z, Hu B and Qiu H 2021. Comprehensive assessment of ecological risk in southwest Guangxi-Beibu bay based on DPSIR model and OWA-GIS. Ecol. Indicat. **132**(22): 334-361.

(Manuscript received on 26 April 2025; revised on 14 October 2025)